Transient Thermoelastic Analysis of a Laminated Hollow Cylinder Constructed of Isotropic Elastic and Magneto-Electro-Thermoelastic Materials

Yoshihiro Ootao[*1], Masayuki Ishihara

Department of Mechanical Engineering, Graduate School of Engineering, Osaka Prefecture University
1-1 Gakuen-cho, Nakaku, Sakai, 599-8531 JAPAN

[*1]ootao@me.osakafu-u.ac.jp

Abstract- **This paper presents the theoretical analysis of a laminated hollow cylinder constructed of isotropic elastic and magneto-electro-thermoelastic materials under unsteady and uniform surface heating. We obtain the exact solution of the transient thermoelastic problem of the laminated hollow cylinder in the plane strain state. As an illustration, we perform numerical calculations of a three-layered composite hollow cylinder made of isotropic elastic, piezoelectric and magnetostrictive materials and investigate the numerical results for temperature change, displacement, stress, and electric and magnetic potential distributions in the transient state.**

Keywords- Thermoelastic Problem; Magneto-Electro-Thermoelastic; Laminated Hollow Cylinder; Plane Strain Problem; Transient State

I. INTRODUCTION

It has recently been found that composites made of piezoelectric and magnetostrictive materials exhibit the magnetoelectric effect, which is not seen in piezoelectric or magnetostrictive materials [1-3]. These materials are known as multiferroic magnetoelectric composites [4]. These composites exhibit new effects, such as a coupling among magnetic, electric, and elastic fields. It is possible to develop a new system of smart composite materials by combining the piezoelectric and magnetostrictive materials with other structural materials.

In the past, various problems in magneto-electro-elastic media that exhibit anisotropic and linear coupling among the magnetic, electric, and elastic fields were analyzed. Examples of static problems are as follows. Pan [5] derived the exact solution of simply supported and multilayered magneto-electro-elastic plates, and Pan and Heyliger [6] derived the exact solution of magneto-electro-elastic laminates in cylindrical bending. Babaei and Chen derived the exact solution of radially polarized and magnetized rotating magneto-electro-elastic hollow and solid cylinders [7]. Ying and Wang derived the exact solution of rotating magneto-electro-elastic composite hollow cylinders [8]. Wang et al. derived an analytical solution of a multilayered magneto-electro-elastic circular plate under simply supported boundary conditions [9]. Examples of dynamic problems are as follows. Wang and Ding analyzed the transient responses of a magneto-electro-elastic hollow sphere [10] and a magneto-electro-elastic composite hollow sphere [11] subjected to spherically symmetric dynamic loads. Anandkumar et al. analyzed the free vibration behavior of multiphase and layered magneto-electro-elastic beams [12]. Huang et al. treated the static analysis of anisotropic functionally graded magneto-electro-elastic beams subjected to arbitrary loading [13]. Wang et al. obtained the three-dimensional exact solutions for free vibrations of simply supported magneto-electro-elastic cylindrical panels [14]. Chu et al. presented a semi-analytical solution for a layered multiferroic half space under a uniform vertical circular load on its surface, analyzed a two-layered system made of $BaTiO_3$ and $CoFeO_4$ [15]. Zhou and Lee obtained the closed-form solutions in contact problem for magneto-electro-elastic half-plane materials indented by a moving punch [16]. Milazzo and Orlando presented a new finite element based upon an elastic equivalent single-layer model for shear deformable and straight magneto-electro-elastic generally laminated beam [17]. Huang and Hu treated a singularity analysis for a magneto-electro-elastic body of revolution, and obtained the three-dimensional asymptotic solutions [18].

Examples of thermal stress problems are as follows. Sunar et al. [19] analyzed thermopiezomagnetic smart structures and Kumarval et al. [20] analyzed a three-layered electro-magneto-elastic strip under steady state conditions using the finite element method. Hou et al. obtained 2D fundamental solutions of a steady point heat source in infinite and semi-infinite orthotropic electro-magneto-thermo-elastic planes [21] and obtained Green's function for a steady point heat source on the surface of a semi-infinite transversely isotropic electro-magneto-thermo-elastic material [22]. Xiong and Ni obtained 2D Green's functions for semi-infinite transversely isotropic electro-magneto-thermo-elastic composites [23]. Rekik et al. treated the axisymmetric problem of a partially insulated mixed-mode crack embedded in a functionally graded pyro magneto-electro-elastic infinite medium subjected to thermal loading [24]. Kondaiah et al. investigated the pyroelectric and pyromagnetic effects on multiphase magneto-electro-elastic cylindrical shells for axisymmetric temperature using semi-analytical finite element procedures [25]. These studies, however, treated thermal stress problems only under steady temperature distribution. It is well known that thermal stress distributions in a transient state show significant and large response values as compared to those in a steady state. Therefore, transient thermoelastic problems are important. With regard to transient thermal stress

problems, Wang and Niraula analyzed transient thermal fracture in transversely isotropic electro-magneto-elastic cylinders [26]. The exact solution of a transient analysis of multilayered magneto-electro-thermoelastic strip subjected to nonuniform heat supply was also obtained [27]. The exact solution of a transient analysis of multilayered magneto-electro-thermoelastic hollow cylinder subjected to uniform heat supply was also obtained [28].

On the other hand, examples concerned smart materials systems are as follows. The piezoelasticity of the laminated piezoelectric structures were reviewed by Saravanos and Heyliger [29]. Analytical studies concerned with piezothermoelasticity of smart composite structures were reviewed by Tauchert et al. [30]. Analytical studies having relevance to control of transient response in smar piezothermoelastic structures were reviewed by Tauchert and Ashida [31]. The transient piezothermoelastic problems in cylindrical composite panels composed of cross-ply/angle-ply and piezoelectric laminae were analyzed exactly [32, 33]. The transient piezothermoelastic problems in laminated hollow cylinder constructed of isotropic elastic and piezoelectric layers due to asymmetrical heating were analyzed exactly [34]. However, to the best of the authors' knowledge, the transient thermoelastic analysis of laminated structures constructed of structural materials and magneto-electro-thermoelastic materials has not yet been reported.

Here, we analyse exactly the transient thermoelasric problem of a laminated hollow cylinder constructed of isotropic elastic and magneto-electro-thermoelastic materials under uniform surface heating in a plane strain state by extending our previous papers [28]. We assumed that the magneto-electro-thermoelastic materials are polarized and magnetized in the radial direction.

II. HEAT CONDUCTION PROBLEM

We considered a laminated hollow cylinder constructed of isotropic elastic and magneto-electro-thermoelastic materials. The laminated hollow cylinder's inner and outer radii are denoted by *a* and *b*, respectively. r_i is the outer radius of the *i*th layer. Throughout this article, indices *i* (=1,2,…, *N*) are associated with the *i*th layer from the inner side of a composite hollow cylinder.

We assumed that the laminated hollow cylinder is initially at zero temperature and its inner and outer surfaces are suddenly heated by surrounding media having constant temperatures T_a and T_b with relative heat transfer coefficients h_a and h_b, respectively. Then, the temperature distribution is one-dimensional, and the transient heat conduction equation for the *i*th layer is written in the following form:

$$\frac{\partial \overline{T}_i}{\partial \tau} = \overline{\kappa}_{ri}\left(\frac{\partial^2 \overline{T}_i}{\partial \overline{r}^2} + \frac{1}{\overline{r}}\frac{\partial \overline{T}_i}{\partial \overline{r}}\right); i = 1, \cdots, N \tag{1}$$

The initial and thermal boundary conditions in dimensionless form are

$$\tau = 0; \quad \overline{T}_i = 0 \quad ; \quad i = 1,2,\cdots,N \tag{2}$$

$$\overline{r} = \overline{a}\,; \ \frac{\partial \overline{T}_1}{\partial \overline{r}} - H_a \overline{T}_1 = -H_a \overline{T}_a \tag{3}$$

$$\overline{r} = R_i\,; \ \overline{T}_i = \overline{T}_{i+1} \quad ; \quad i = 1,2,\cdots,N-1 \tag{4}$$

$$\overline{r} = R_i; \overline{\lambda}_{ri}\frac{\partial \overline{T}_i}{\partial \overline{r}} = \overline{\lambda}_{r,i+1}\frac{\partial \overline{T}_{i+1}}{\partial \overline{r}} \ ; \ i = 1,2,\cdots,N-1 \tag{5}$$

$$\overline{r} = 1; \ \frac{\partial \overline{T}_N}{\partial \overline{r}} + H_b \overline{T}_N = H_b \overline{T}_b \tag{6}$$

In Eqs. (1)-(6), we introduced the following dimensionless values:

$$\begin{aligned} &(\overline{T}_i, \overline{T}_a, \overline{T}_b) = (T_i, T_a, T_b)/T_0\ , (\overline{r}, R_i, \overline{a}) = (r, r_i, a)/b\ , \tau = \kappa_0 t/b^2\ , \overline{\kappa}_{ri} = \kappa_{ri}/\kappa_0 \\ &\overline{\lambda}_{ri} = \lambda_{ri}/\lambda_0\ , \ (H_a, H_b) = (h_a, h_b)b \end{aligned} \tag{7}$$

where T_i is the temperature change; t is time; and T_0, λ_0 and κ_0 are typical values of temperature, thermal conductivity, and thermal diffusivity, respectively. Introducing the Laplace transform with respect to the variable τ, the solution of Eq. (1) can be obtained so as to satisfy the Conditions (2)-(6). This solution is written as follows:

$$\overline{T}_i = \frac{1}{F}(\overline{A}_i' + \overline{B}_i' \ln \overline{r}) + \sum_{j=1}^{\infty} \frac{2\exp(-\mu_j^2 \tau)}{\mu_j \Delta'(\mu_j)}[\overline{A}_i J_0(\beta_i \mu_j \overline{r}) + \overline{B}_i Y_0(\beta_i \mu_j \overline{r})]; \ i = 1,2,\cdots,N \tag{8}$$

where $J_0(\,)$ and $Y_0(\,)$ are zeroth-order Bessel functions of the first and second kind, respectively. Futhermore, Δ and F are the determinants of $2N \times 2N$ matrices [*akl*] and [*ekl*], respectively; the coefficients $\overline{A}_i$ and $\overline{B}_i$ are defined as determinants of a

matrix similar to the coefficient matrix [*akl*], in which the (2*i*-1)th column or 2*i*th column is replaced with the constant vector $\{c_k\}$, respectively. Similarly, the coefficients $\bar{A}_i'$ and $\bar{B}_i'$ are defined as determinants of a matrix similar to the coefficient matrix [*ekl*], in which the (2*i*-1)th column or 2*i*th column is replaced with the constant vector $\{c_k\}$, respectively. The nonzero elements of the coefficient matrices [*akl*] and [*ekl*] and the constant vector $\{c_k\}$ are given

$$\begin{aligned} &a_{1,1} = \beta_1\mu J_1(\beta_1\mu\bar{a}) + H_a J_0(\beta_1\mu\bar{a}),\ a_{1,2} = \beta_1\mu Y_1(\beta_1\mu\bar{a}) + H_a Y_0(\beta_1\mu\bar{a}),\\ &a_{2N,2N-1} = H_b J_0(\beta_N\mu) - \beta_N\mu J_1(\beta_N\mu),\ a_{2N,2N-1} = H_b Y_0(\beta_N\mu) - \beta_N\mu Y_1(\beta_N\mu) \end{aligned} \tag{9}$$

$$\begin{aligned} &a_{2i,2i-1} = J_0(\beta_i\mu R_i),\ a_{2i,2i} = Y_0(\beta_i\mu R_i),\ a_{2i,2i+1} = -J_0(\beta_{i+1}\mu R_i),\ a_{2i,2i+2} = -Y_0(\beta_{i+1}\mu R_i),\\ &a_{2i+1,2i-1} = -\bar{\lambda}_{ri}\beta_i\mu J_1(\beta_i\mu R_i),\ a_{2i+1,2i} = -\bar{\lambda}_{ri}\beta_i\mu Y_1(\beta_i\mu R_i),\ a_{2i+1,2i+1} = \bar{\lambda}_{r,i+1}\beta_{i+1}\mu J_1(\beta_{i+1}\mu R_i)\\ &a_{2i+1,2i+2} = \bar{\lambda}_{r,i+1}\beta_{i+1}\mu Y_1(\beta_{i+1}\mu R_i);\ \ i = 1,2,\cdots,N-1 \end{aligned} \tag{10}$$

$$e_{1,1} = H_a,\ e_{1,2} = H_a\ln\bar{a} - \frac{1}{\bar{a}},\ e_{2N,2N-1} = H_b,\ e_{2N,2N} = 1 \tag{11}$$

$$e_{2i,2i-1} = 1,\ e_{2i,2i} = \ln R_i,\ e_{2i,2i+1} = -1,\ e_{2i,2i+2} = -\ln R_i,\ \ e_{2i+1,2i} = \frac{\bar{\lambda}_{ri}}{R_i},\ e_{2i+1,2i+1} = -\frac{\bar{\lambda}_{r,i+1}}{R_i};\ \ i = 1,2,\cdots,N-1 \tag{12}$$

$$c_1 = H_a\bar{T}_a,\ c_{2N} = H_b\bar{T}_b \tag{13}$$

In Eq. (8), $\Delta'(\mu_j)$ and β_i are

$$\Delta'(\mu_j) = \left.\frac{d\Delta}{d\mu}\right|_{\mu=\mu_j},\ \ \beta_i = \frac{1}{\sqrt{\bar{\kappa}_{ri}}} \tag{14}$$

and μ_j is the *j*th positive root of the following transcendental equation

$$\Delta(\mu) = 0 \tag{15}$$

III. THE RMOELASTIC PROBLEM

We developed the analysis of a laminated hollow cylinder constructed of isotropic elastic and magneto-electro-thermoelastic materials as a plane strain problem. The displacement-strain relations are expressed in dimensionless form as follows:

$$\bar{\varepsilon}_{rri} = \bar{u}_{ri,\bar{r}},\ \bar{\varepsilon}_{\theta\theta i} = \bar{u}_{ri}/\bar{r},\ \bar{\varepsilon}_{zzi} = \bar{\varepsilon}_{r\theta i} = \bar{\varepsilon}_{rzi} = \bar{\varepsilon}_{\theta zi} = 0 \tag{16}$$

where the comma denotes partial differentiation with respect to the variable that follows. For the anisotropic and linear magneto-electro-thermoelastic material, the constitutive relations are expressed in dimensionless form as follows [26]:

$$\begin{aligned} &\bar{\sigma}_{rri} = \bar{C}_{11i}\bar{\varepsilon}_{rri} + \bar{C}_{12i}\bar{\varepsilon}_{\theta\theta i} - \bar{\beta}_{ri}\bar{T}_i - \bar{e}_{1i}\bar{E}_{ri} - \bar{q}_{1i}\bar{H}_{ri},\\ &\bar{\sigma}_{\theta\theta i} = \bar{C}_{12i}\bar{\varepsilon}_{rri} + \bar{C}_{22i}\bar{\varepsilon}_{\theta\theta i} - \bar{\beta}_{\theta i}\bar{T}_i - \bar{e}_{2i}\bar{E}_{ri} - \bar{q}_{2i}\bar{H}_{ri},\\ &\bar{\sigma}_{zzi} = \bar{C}_{13i}\bar{\varepsilon}_{rri} + \bar{C}_{23i}\bar{\varepsilon}_{\theta\theta i} - \bar{\beta}_{zi}\bar{T}_i - \bar{e}_{3i}\bar{E}_{ri} - \bar{q}_{3i}\bar{H}_{ri} \end{aligned} \tag{17}$$

where

$$\bar{\beta}_{ri} = \bar{C}_{11i}\bar{\alpha}_{ri} + \bar{C}_{12i}\bar{\alpha}_{\theta i} + \bar{C}_{13i}\bar{\alpha}_{zi},\ \bar{\beta}_{\theta i} = \bar{C}_{12i}\bar{\alpha}_{ri} + \bar{C}_{22i}\bar{\alpha}_{\theta i} + \bar{C}_{23i}\bar{\alpha}_{zi},\ \bar{\beta}_{zi} = \bar{C}_{13i}\bar{\alpha}_{ri} + \bar{C}_{23i}\bar{\alpha}_{\theta i} + \bar{C}_{33i}\bar{\alpha}_{zi} \tag{18}$$

The constitutive equations for the electric and the magnetic fields in dimensionless form are given as

$$\begin{aligned} &\bar{D}_{ri} = \bar{e}_{1i}\bar{\varepsilon}_{rri} + \bar{e}_{2i}\bar{\varepsilon}_{\theta\theta i} + \bar{\eta}_{1i}\bar{E}_{ri} + \bar{d}_{1i}\bar{H}_{ri} + \bar{p}_{1i}\bar{T}_i,\\ &\bar{B}_{ri} = \bar{q}_{1i}\bar{\varepsilon}_{rri} + \bar{q}_{2i}\bar{\varepsilon}_{\theta\theta i} + \bar{d}_{1i}\bar{E}_{ri} + \bar{\mu}_{1i}\bar{H}_{ri} + \bar{m}_{1i}\bar{T}_i, \end{aligned} \tag{19}$$

The relation between the electric field intensity and the electric potential ϕ_i in dimensionless form is defined as

$$\bar{E}_{ri} = -\bar{\phi}_{i,\bar{r}} \tag{20}$$

The relation between the magnetic field intensity and the magnetic potential ψ_i in dimensionless form is defined as

$$\overline{H}_{ri} = -\overline{\psi}_{i,\bar{r}} \tag{21}$$

The equilibrium equation is expressed in dimensionless form as follows:

$$\overline{\sigma}_{rri,\bar{r}} + (\overline{\sigma}_{rri} - \overline{\sigma}_{\theta\theta i})/\bar{r} = 0 \tag{22}$$

If the electric charge density is zero, the equations of electrostatics and magnetostatics are expressed in dimensionless form as follows:

$$\overline{D}_{ri,\bar{r}} + \overline{D}_{ri}/\bar{r} = 0 \tag{23}$$

$$\overline{B}_{ri,\bar{r}} + \overline{B}_{ri}/\bar{r} = 0 \tag{24}$$

In Eqs. (16)-(24), the following dimensionless values are introduced:

$$\overline{\sigma}_{kli} = \frac{\sigma_{kli}}{\alpha_0 Y_0 T_0},\ \overline{\varepsilon}_{kli} = \frac{\varepsilon_{kli}}{\alpha_0 T_0},\ \overline{u}_{ri} = \frac{u_{ir}}{\alpha_0 T_0 b},\ \overline{\alpha}_{ki} = \frac{\alpha_{ki}}{\alpha_0},\ \overline{C}_{kli} = \frac{C_{kli}}{Y_0},\ \overline{D}_{ri} = \frac{D_{ri}}{\alpha_0 Y_0 T_0 |d_0|},\ \overline{B}_{ri} = \frac{B_{ri}|d_0|\kappa_0}{b\alpha_0 T_0},$$

$$\overline{\phi}_i = \frac{\phi_i |d_0|}{\alpha_0 T_0 b},\ \overline{\psi}_i = \frac{\psi_i}{|d_0|\kappa_0\alpha_0 Y_0 T_0},\ \overline{e}_{ki} = \frac{e_{ki}}{Y_0|d_0|},\ \overline{\eta}_{1i} = \frac{\eta_{1i}}{Y_0|d_0|^2},\ \overline{q}_{ki} = \frac{q_{ki}\kappa_0|d_0|}{b},\ \overline{\mu}_{1i} = \frac{\mu_{1i}\kappa_0^2|d_0|^2 Y_0}{b^2},$$

$$\overline{d}_{1i} = \frac{\kappa_0 d_{1i}}{b},\ \overline{p}_{1i} = \frac{p_{1i}}{\alpha_0 Y_0 |d_0|},\ \overline{m}_{1i} = \frac{m_{1i}\kappa_0|d_0|}{b\alpha_0},\ \overline{E}_{ri} = \frac{E_{ri}|d_0|}{\alpha_0 T_0},\ \overline{H}_{ri} = \frac{H_{ri} b}{|d_0|\kappa_0\alpha_0 Y_0 T_0} \tag{25}$$

where σ_{kli} are the stress components; ε_{kli} are the strain components; u_{ri} is the displacement in the *r* direction; α_{ki} are the coefficients of linear thermal expansion; C_{kli} are the elastic stiffness constants; D_{ri} is the electric displacement in the *r* direction; B_{ri} is the magnetic flux density in the *r* direction; e_{ki} are the piezoelectric coefficients; η_{1i} is the dielectric constant; p_{1i} is the pyroelectric constant; q_{ki} are the piezomagnetic coefficients; μ_{1i} is the magnetic permeability coefficient; d_{1i} is the magnetoelectric coefficient; m_{1i} is the pyromagnetic constant; and α_0, Y_0 and d_0 are typical values of the coefficient of linear thermal expansion, Young's modulus, and piezoelectric modulus, respectively.

Substituting Eqs. (16), (20), and (21) into Eqs. (17), and (19) and later into Eqs. (22)-(24), the governing equations of the displacement u_{ri}, electric potential ϕ_i, and magnetic potential ψ_i in the dimensionless form are written as

$$\begin{aligned}&\overline{C}_{11i}\overline{u}_{ri,\bar{r}\bar{r}} + \overline{C}_{11i}\overline{u}_{ri,\bar{r}}\,\bar{r}^{-1} - \overline{C}_{22i}\overline{u}_{ri}\bar{r}^{-2} + \overline{e}_{1i}\overline{\phi}_{i,\bar{r}\bar{r}} + (\overline{e}_{1i} - \overline{e}_{2i})\overline{\phi}_{i,\bar{r}}\,\bar{r}^{-1} + \overline{q}_{1i}\overline{\psi}_{i,\bar{r}\bar{r}} + (\overline{q}_{1i} - \overline{q}_{2i})\overline{\psi}_{i,\bar{r}}\,\bar{r}^{-1} \\ &\quad = (\overline{\beta}_{ri} - \overline{\beta}_{\theta i})\overline{T}_i\bar{r}^{-1} + \overline{\beta}_{ri}\overline{T}_{i,\bar{r}}\end{aligned} \tag{26}$$

$$\overline{e}_{1i}\overline{u}_{ri,\bar{r}\bar{r}} + (\overline{e}_{1i} + \overline{e}_{2i})\overline{u}_{ri,\bar{r}}\,\bar{r}^{-1} - \overline{\eta}_{1i}\overline{\phi}_{i,\bar{r}\bar{r}} - \overline{\eta}_{1i}\overline{\phi}_{i,\bar{r}}\,\bar{r}^{-1} - \overline{d}_{1i}\overline{\psi}_{i,\bar{r}\bar{r}} - \overline{d}_{1i}\overline{\psi}_{i,\bar{r}}\,\bar{r}^{-1} = -\overline{p}_{1i}(\overline{T}_{i,\bar{r}} + \overline{T}_i\bar{r}^{-1}) \tag{27}$$

$$\overline{q}_{1i}\overline{u}_{ri,\bar{r}\bar{r}} + (\overline{q}_{1i} + \overline{q}_{2i})\overline{u}_{ri,\bar{r}}\,\bar{r}^{-1} - \overline{d}_{1i}\overline{\phi}_{i,\bar{r}\bar{r}} - \overline{d}_{1i}\overline{\phi}_{i,\bar{r}}\,\bar{r}^{-1} - \overline{\mu}_{1i}\overline{\psi}_{i,\bar{r}\bar{r}} - \overline{\mu}_{1i}\overline{\psi}_{i,\bar{r}}\,\bar{r}^{-1} = -\overline{m}_{1i}(\overline{T}_{i,\bar{r}} + \overline{T}_i\bar{r}^{-1}) \tag{28}$$

The solutions of Eqs. (26)-(28) are assumed in the following form:

$$\overline{u}_{ri} = \overline{u}_{rci} + \overline{u}_{rpi},\ \overline{\phi}_i = \overline{\phi}_{ci} + \overline{\phi}_{pi},\ \overline{\psi}_i = \overline{\psi}_{ci} + \overline{\psi}_{pi} \tag{29}$$

In Eq. (29), the first term on the right-hand side gives the homogeneous solution and the second term gives the particular solution. The homogeneous solutions of Eq. (29) can be expressed as follows:

$$\begin{aligned}&\overline{u}_{rci} = C_{1i}\bar{r}^{-1} + C_{3i}\bar{r}^{m_i} + C_{4i}\bar{r}^{-m_i}, \\ &\overline{\phi}_{ci} = \frac{\overline{C}_{11i}}{\overline{e}_{1i}}(C_{8i} + C_{7i}\ln\bar{r} + g_{5i}C_{3i}\bar{r}^{m_i} + g_{6i}C_{4i}\bar{r}^{-m_i}), \\ &\overline{\phi}_{ci} = \frac{\overline{C}_{11i}}{\overline{e}_{1i}}(C_{8i} + C_{7i}\ln\bar{r} + g_{5i}C_{3i}\bar{r}^{m_i} + g_{6i}C_{4i}\bar{r}^{-m_i}),\end{aligned} \tag{30}$$

where

$$m_i=\sqrt{-\frac{b_{2i}}{b_{4i}}},\ b_{2i}=-[\alpha_i\gamma_i+\beta_{ei}^2+\frac{(\beta_{qi}\gamma_i-\beta_{ei}\beta_{di})^2}{\delta_i\gamma_i-\beta_{di}^2}],\ b_{4i}=1+\gamma_i+\frac{(\gamma_i-\beta_{di})^2}{\delta_i\gamma_i-\beta_{di}^2},\ \alpha_i=\frac{\overline{C}_{22i}}{\overline{C}_{11i}},\ \beta_{ei}=\frac{\overline{e}_{2i}}{\overline{e}_{1i}},\ \beta_{qi}=\frac{\overline{q}_{2i}}{\overline{q}_{1i}},$$

$$\beta_{di}=\frac{\overline{C}_{11i}\overline{d}_{1i}}{\overline{e}_{1i}\overline{q}_{1i}},\ \overline{\gamma}_i=\frac{\overline{C}_{11i}\overline{\eta}_{1i}}{\overline{e}_{1i}^2},\ \delta_i=\frac{\overline{C}_{11i}\overline{\mu}_{1i}}{\overline{q}_{1i}^2},\ g_{5i}=\frac{1}{m_i\gamma_i}[m_i(1-g_{2i}\beta_{di})+\beta_{ei}],$$

$$g_{6i}=\frac{1}{m_i\gamma_i}[m_i(1-g_{3i}\beta_{di})-\beta_{ei}],\ g_{2i}=\frac{1}{m_i(\delta_i\gamma_i-\beta_{di}^2)}[m_i(\gamma_i-\beta_{di})+\beta_{qi}\gamma_i-\beta_{ei}\beta_{di}],$$

$$g_{3i}=\frac{1}{m_i(\delta_i\gamma_i-\beta_{di}^2)}[m_i(\gamma_i-\beta_{di})-\beta_{qi}\gamma_i+\beta_{ei}\beta_{di}] \tag{31}$$

In Eq. (31), C_{ki} ($k=1,3\cdots,8$) are unknown constants. We have the following relation.

$$\alpha_iC_{1i}+\beta_{ei}C_{7i}+\beta_{qi}C_{5i}=0 \tag{32}$$

In order to obtain the particular solutions, series expansions of Bessel functions given in Eq. (8) are used [35]. Eq. (8) can be written in the following way:

$$\overline{T}_i(\bar{r}_i,\tau)=\sum_{n=0}^{\infty}[a_{in}(\tau)\bar{r}^{2n}+b_{in}(\tau)\bar{r}^{2n}\ln\bar{r}] \tag{33}$$

where

$$a_{in}(\tau)=\frac{\overline{A}_i'}{F}\delta_{0n}+\sum_{j=1}^{\infty}\frac{2\exp(-\mu_j^2\tau)}{\mu_j\Delta'(\mu_j)}[\overline{A}_i+\frac{2}{\pi}\overline{B}_i(\gamma^*+\ln\frac{\beta_i\mu_j}{2}-\sum_{m=1}^{n}\frac{1}{m})]\frac{(-1)^n}{n!n!}\left(\frac{\beta_i\mu_j}{2}\right)^{2n} \tag{34}$$

$$b_{in}(\tau)=\frac{\overline{B}_i'}{F}\delta_{0n}+\sum_{j=1}^{\infty}\frac{2\exp(-\mu_j^2\tau)}{\mu_j\Delta'(\mu_j)}\frac{2}{\pi}\overline{B}_i\frac{(-1)^n}{n!n!}\left(\frac{\beta_i\mu_j}{2}\right)^{2n} \tag{35}$$

Here, δ_{0n} is the Kronecker delta, and γ^* is Euler's constant. The particular solutions $\overline{u}_{rpi},\overline{\phi}_{pi}$, and $\overline{\psi}_{pi}$ are obtained as the function system like Eq. (33). Then, the stress components, electric displacement, and magnetic flux density can be evaluated from Eq. (29). Details of the solutions are omitted from here for brevity.

For the isotropic elastic material, we analyze by using Airy stress function method. The solutions of displacement and stress components can be expressed as follows [36]:

$$\begin{aligned}&\overline{u}_{ri}=\frac{\bar{r}}{\overline{E}_i}(1+\nu_i)[\overline{k}_iD_i(\bar{r})+(1-2\nu_i)C_{i2}'-\frac{1}{\bar{r}^2}C_{i3}'],\\&\overline{\sigma}_{rri}=-\overline{k}_iD_i(\bar{r})+C_{i2}'+\frac{1}{\bar{r}^2}C_{i3}',\ \overline{\sigma}_{rri}=\overline{k}_iD_i(\bar{r})-\overline{k}_i\overline{T}_i+C_{i2}'-\frac{1}{\bar{r}^2}C_{i3}',\\&\overline{\sigma}_{zzi}=\nu_i(\overline{\sigma}_{rri}+\overline{\sigma}_{\theta\theta i})-\overline{\alpha}_i\overline{Y}_i\overline{T}_i\end{aligned} \tag{36}$$

where

$$D_i(\bar{r})=\frac{1}{\bar{r}}\int\overline{T}_i\bar{r}d\bar{r},\ \overline{k}_i=\frac{\overline{\alpha}_i\overline{Y}_i}{1-\nu_i} \tag{37}$$

In Eq. (36), C_{i2}' and C_{i3}' are unknown constants. In Eqs. (36) and (37), α_i is the coefficient of linear thermal expansion; Y_i is Young's modulus; and ν_i is Poisson's ratio. The following dimensionless values are introduced:

$$\overline{\alpha}_i=\frac{\alpha_i}{\alpha_0},\ \overline{Y}_i=\frac{Y_i}{Y_0} \tag{38}$$

If the inner and outer surfaces of the laminated hollow cylinder are traction free, and the interfaces of each adjoining layer are perfectly bonded, then the boundary conditions of inner and outer surfaces and the conditions of continuity at the interfaces can be represented as follows:

$$\begin{aligned}
&\bar{r} = \bar{a}\,;\ \bar{\sigma}_{rr1} = 0\,,\\
&\bar{r} = R_i\,;\ \ \bar{\sigma}_{rri} = \bar{\sigma}_{rr,i+1},\ \bar{u}_{ri} = \bar{u}_{r,i+1}\ ;i = 1,\cdots,N-1\,,\\
&\bar{r} = 1;\ \ \bar{\sigma}_{rrN} = 0
\end{aligned} \tag{39}$$

For example, when the *N*th layer is a isotropic elastic layer, the boundary conditions in the radial direction for the electric and magnetic fields are expressed as

$$\begin{aligned}
&\bar{r} = \bar{a}\,;\ \ \bar{D}_{r1} = 0, \bar{B}_{r1} = 0 \text{ or } \bar{\phi}_1 = 0, \bar{\psi}_1 = 0\,,\\
&\bar{r} = R_i\,;\ \ \bar{D}_{ri} = \bar{D}_{r,i+1}, \bar{B}_{ri} = \bar{B}_{r,i+1},\ \bar{\phi}_i = \bar{\phi}_{i+1},\ \bar{\psi}_i = \bar{\psi}_{i+1}\ ;i = 1,\cdots,N-2\,,\\
&\bar{r} = R_{N-1};\ \ \bar{\phi}_N = 0, \bar{\psi}_N = 0
\end{aligned} \tag{40}$$

The unknown constants in Eqs. (30) and (36) are determined so as to satisfy the boundary conditions in (39) and (40).

IV. NUMERICAL RESULTS

In order to illustrate the foregoing analysis, we consider a three-layered hollow cylinder composed of isotropic elastic, piezoelectric and magnetostrictive layers. The isotropic elastic layer is made up of mild steel, the piezoelectric layer is made up of $BaTiO_3$, and the magnetostrictive layer is made up of $CoFe_2O_4$. Two kinds of three-layered hollow cylinders are investigated. Case 1 shows the stacking sequence $BaTiO_3/CoFe_2O_4$/(mild steel) and Case 2 shows the stacking sequence $CoFe_2O_4/BaTiO_3$/(mild steel). We assume that the outer surface of the three-layered hollow cylinder is heated. Then, numerically calculable parameters of the heat condition and shape are presented as follows:

$$\begin{aligned}
&H_a = H_b = 1.0,\ \bar{T}_a = 0,\ \ \bar{T}_b = 1,\ N = 3,\\
&\bar{a} = 0.7,\ R_1 = 0.71, 0.73, 0.75, 0.77, 0.79,\ R_2 = 0.8,\ b = 0.01m
\end{aligned} \tag{41}$$

The following are material constants considered for mild steel [37]:

$$\lambda = 51.6\,W/mK,\ \kappa = 13.88\times10^{-6}\ m^2/s,\ \alpha = 11.8\times10^{-6}1/K,\ Y = 206GPa,\ \nu = 0.3 \tag{42}$$

The following are material constants considered for $BaTiO_3$ [2, 5, 27]:

$$\begin{aligned}
&\alpha_\theta = \alpha_z = 15.7\times10^{-6}1/K,\ \alpha_r = 6.4\times10^{-6}1/K,\ \ C_{22} = C_{33} = 166GPa,\ C_{23} = 77GPa,\ C_{12} = C_{13} = 78GPa,\\
&C_{11} = 162GPa,\ \ e_2 = e_3 = -4.4C/m^2,\ e_1 = 18.6C/m^2,\ \eta_1 = 12.6\times10^{-9}C^2/Nm^2,\\
&p_1 = 2\times10^{-4}C^2/m^2K,\ \mu_1 = 10\times10^{-6}Ns^2/C^2,\ \lambda_r = 2.5\,W/mK,\ \kappa_r = 0.88\times10^{-6}\ m^2/s
\end{aligned} \tag{43}$$

The corresponding constants for $CoFe_2O_4$ [5, 27] are

$$\begin{aligned}
&\alpha_r = \alpha_\theta = \alpha_z = 10\times10^{-6}1/K,\ C_{22} = C_{33} = 286GPa,\ \ C_{23} = 173GPa,\ C_{12} = C_{13} = 170.5GPa,\\
&C_{11} = 269.5GPa,\ \ q_2 = q_3 = 580.3N/Am,\ q_1 = 699.7\,N/Am,\ \eta_1 = 0.093\times10^{-9}C^2/Nm^2,\\
&p_1 = 2\times10^{-4}C^2/m^2K,\ \mu_1 = 157\times10^{-6}Ns^2/C^2,\ \lambda_r = 3.2\,W/mK,\ \ \kappa_r = 0.77\times10^{-6}\ m^2/s
\end{aligned} \tag{44}$$

The typical values of material parameters such as κ_0, λ_0, α_0, Y_0, and d_0, used to normalize the numerical data, based on those of $BaTiO_3$ are as follows:

$$\kappa_0 = \kappa_r,\ \lambda_0 = \lambda_r,\ \alpha_0 = \alpha_r,\ Y_0 = 116GPa,\ d_0 = -78\times10^{-12}C/N \tag{45}$$

In the numerical calculations, the boundary conditions at the surfaces for the electric and magnetic fields are expressed as

$$\bar{r} = \bar{a}\,;\ \ \bar{D}_{r1} = 0, \bar{B}_{r1} = 0 \tag{46}$$

The numerical results for Case 1 and $R_1 = 0.75$ are shown in Figs. 1-4. Fig. 1 shows the variation of temperature change along the radial direction. Fig. 2 shows the variation of displacement $\bar{u}_r$ along the radial direction. From Figs. 1 and 2, it is clear that the temperature and displacement increase with time and have the largest values in steady state. Figs. 3(a), (b) and (c) show variations of thermal stresses $\bar{\sigma}_{rr}$, $\bar{\sigma}_{\theta\theta}$, and $\bar{\sigma}_{zz}$, respectively, along the radial direction. Fig. 3(a) reveals that the maximum tensile stress occurs in the transient state and the maximum compressive stress occurs in the steady state. From Fig. 3(b), it is clear that the compressive stress occurs in the first layer and tensile stress occurs in the second layer. From Fig. 3(c), it is clear that the compressive stress occurs inside the hollow cylinder and its absolute value increases with time. Figs. 4(a) and

4(b) show variations of electric potential $\bar{\phi}$ and magnetic potential $\bar{\psi}$, respectively, along the radial direction. Fig. 4 reveals that the absolute value of the electric and magnetic potential increases with time and attains its maximum value in the steady state. The electric potential is almost zero in the second layer, i.e. the magnetostrictive layer. The magnetic potential is almost constant in the first layer, i.e. the piezoelectric layer.

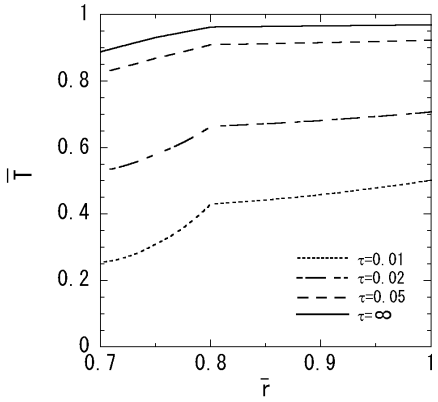

Fig. 1 Variation of temperature change in the radial direction (Case 1, $R_1 = 0.75$)

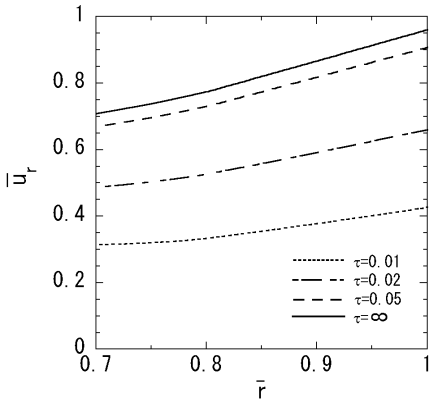

Fig. 2 Variation of displacement $\bar{u}_r$ in the radial direction (Case 1, $R_1 = 0.75$)

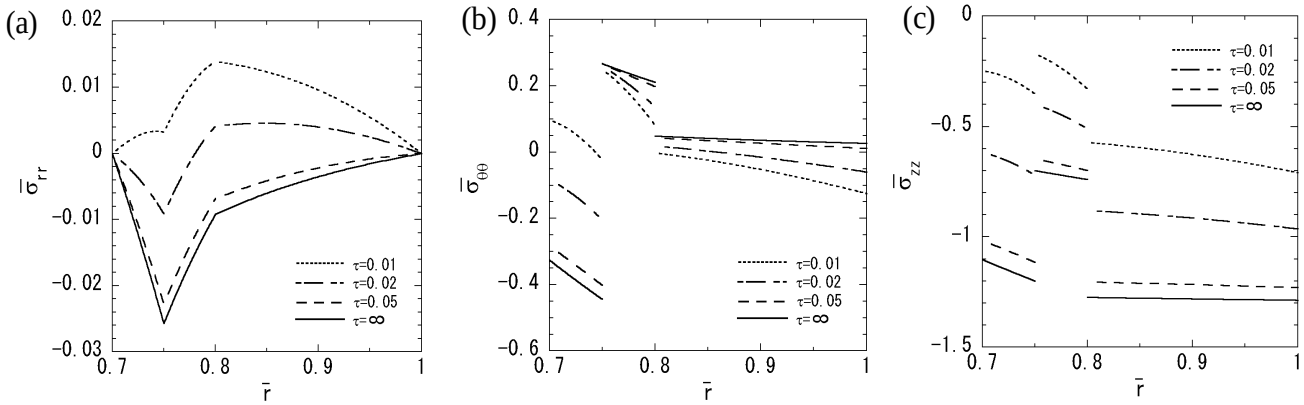

Fig. 3 Variation of thermal stresses in the radial direction (Case 1, $R_1 = 0.75$): (a) normal stress $\bar{\sigma}_{rr}$ (b) normal stress $\bar{\sigma}_{\theta\theta}$ and (c) normal stress $\bar{\sigma}_{zz}$

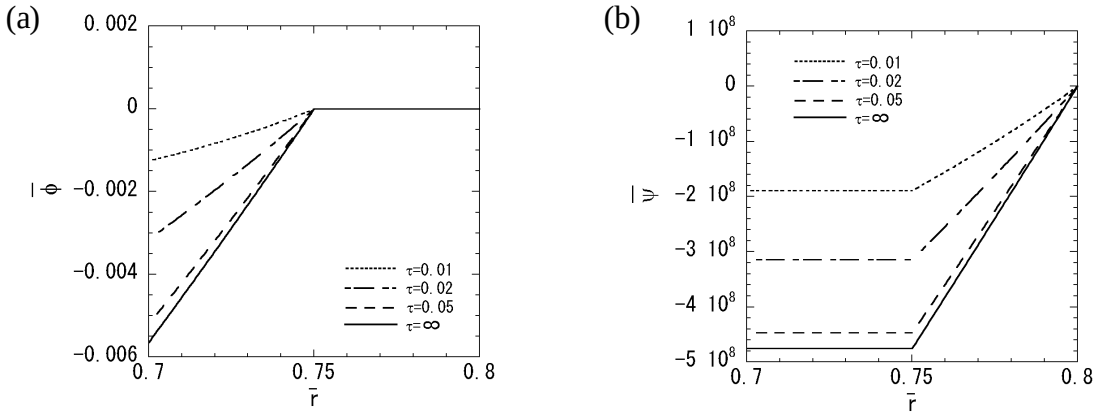

Fig. 4 Variation of (a) electric potential and (b) magnetic potential in the radial direction (Case 1, $R_1 = 0.75$)

The numerical results for Case 2 and $R_1 = 0.75$ are shown in Figs. 5-8. Fig. 5 shows the variation of temperature change along the radial direction. Fig. 6 shows the variation of displacement $\bar{u}_r$ along the radial direction. From Figs. 1, 2, 5, and 6, there is little difference between Case 1 and Case 2 for the temperature change and displacement $\bar{u}_r$. Figs. 7(a), (b) and (c) show the variations of thermal stresses $\bar{\sigma}_{rr}$, $\bar{\sigma}_{\theta\theta}$, and $\bar{\sigma}_{zz}$, respectively, along the radial direction. From Fig. 7(a), it is clear that

the maximum tensile stress occurs between the first layer and the second layer. Fig. 7(b) reveals that maximum tensile stress occurs in the first layer and maximum compressive stress occurs in the second layer. Fig. 7(c) reveals that compressive stress occurs inside the hollow cylinder and its absolute value increases with time. The maximum compressive stress occurs in the third layer. Figs. 8(a) and 8(b) show the variations of electric potential $\bar{\phi}$ and magnetic potential $\bar{\psi}$, respectively, along the radial direction. From these figures, it is clear that the absolute values of the electric and magnetic potential increases with time, and attain their maximum value in the steady state. The electric potential is almost constant in the first layer, i.e. the magnetostrictive layer. In contrast, the magnetic potential is almost zero in the second layer, i.e. the piezoelectric layer.

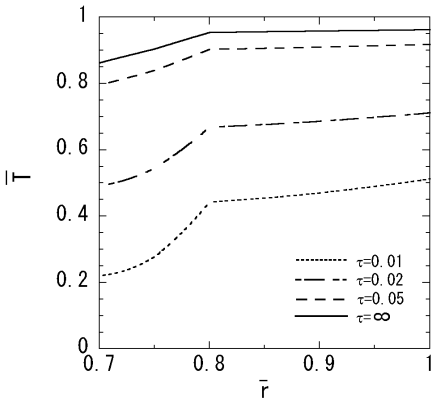

Fig. 5 Variation of temperature change in the radial direction (Case 2, $R_1 = 0.75$)

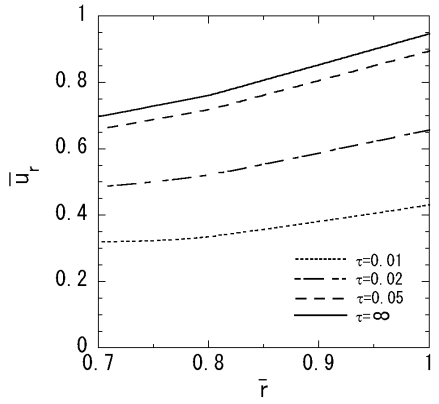

Fig. 6 Variation of displacement $\bar{u}_r$ in the radial direction (Case 2, $R_1 = 0.75$)

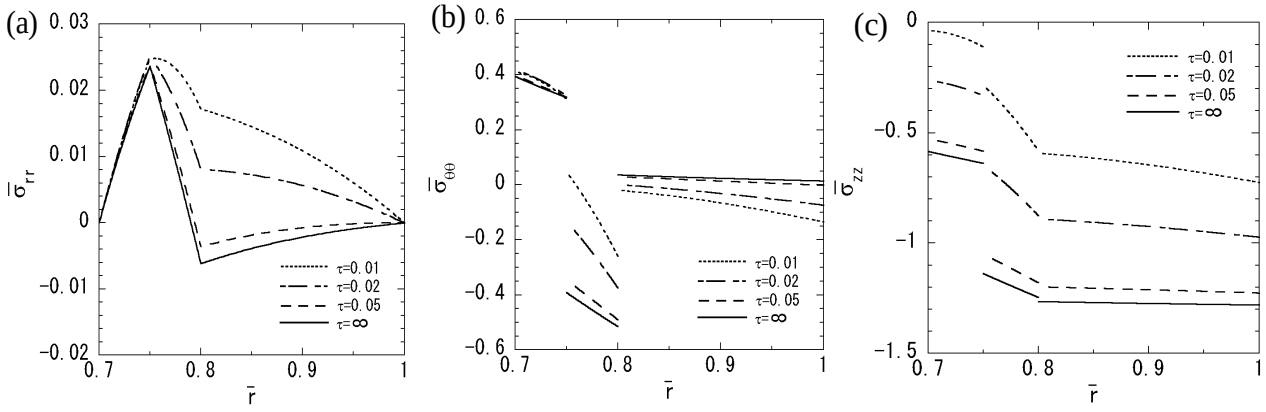

Fig. 7 Variation of thermal stresses in the radial direction (Case 2, $R_1 = 0.75$): (a) normal stress $\bar{\sigma}_{rr}$ (b) normal stress $\bar{\sigma}_{\theta\theta}$ and (c) normal stress $\bar{\sigma}_{zz}$

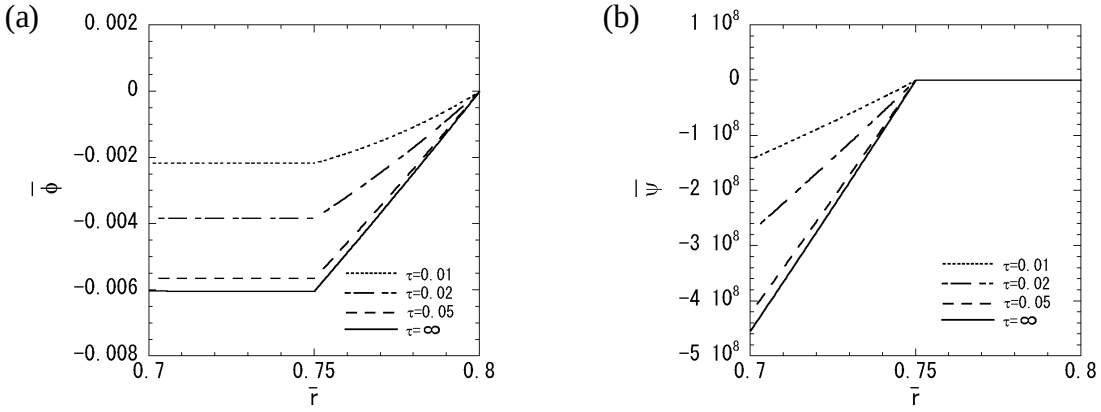

Fig. 8 Variation of (a) electric potential and (b) magnetic potential in the radial direction (Case 2, $R_1 = 0.75$)

In order to assess the influence of the position of the interface between the first layer and the second layer, numerical results for case 1 and $R_1 = 0.71, 0.73, 0.75, 0.77, 0.79$ were obtained; these results are shown in Figs. 9 and 10. Figs. 9(a) and (b)

show the variations of thermal stresses $\bar{\sigma}_{rr}$ and $\bar{\sigma}_{\theta\theta}$, respectively, in the steady state. Figs. 10(a) and (b) show the variations of electric and magnetic potential, respectively, in the steady state. From Figs. 9(a) and (b), it is clear that the distribution of the thermal stress $\bar{\sigma}_{rr}$ changes substantially with a change in the parameter R_1, whereas the maximum tensile stress $\bar{\sigma}_{\theta\theta}$ increases with an increase R_1. It can be seen from Figs. 10(a) and (b) that the absolute values of electric potential increase and those of magnetic potential decrease with an increase in R_1.

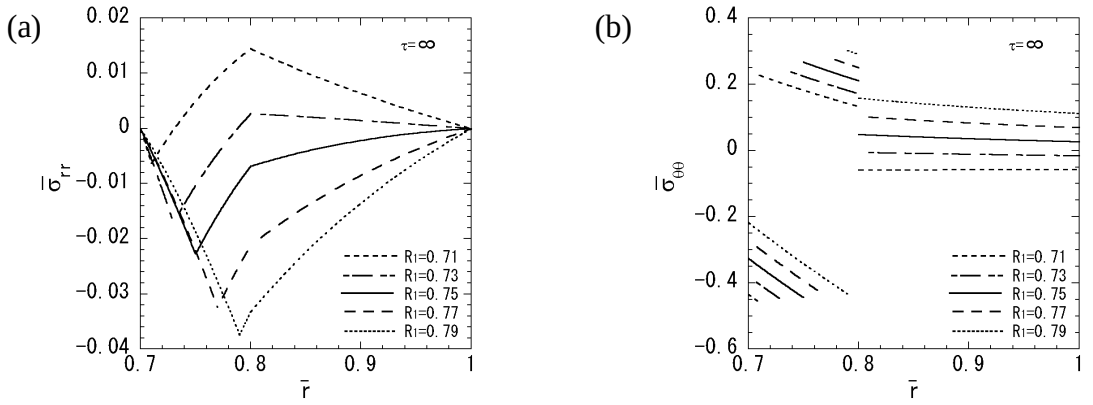

Fig. 9 Variation of thermal stresses in the radial direction (Case 1, $\tau = \infty$): (a) normal stress $\bar{\sigma}_{rr}$ and (b) normal stress $\bar{\sigma}_{\theta\theta}$

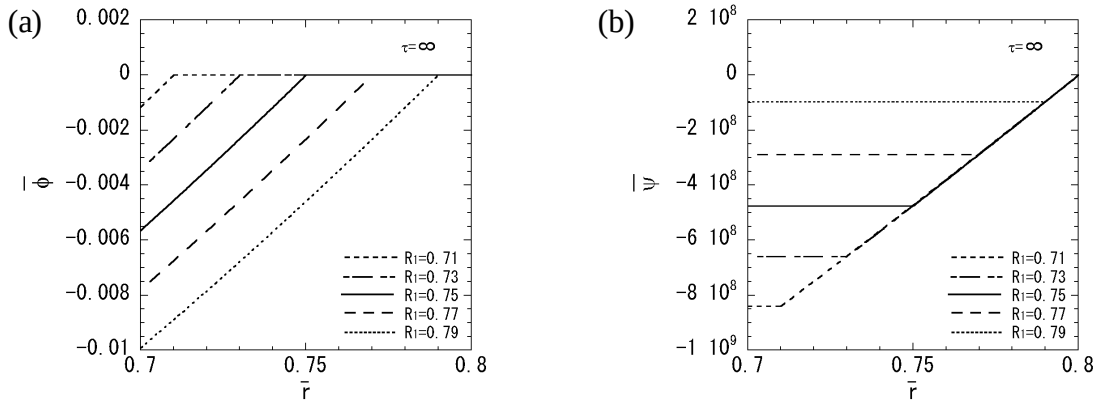

Fig. 10 Variation of (a) electric potential and (b) magnetic potential in the radial direction (Case 1, $\tau = \infty$)

In order to examine the convergence of the series expansions of Bessel functions, the influence of the upper limit ($\equiv n_{\max}$) of series of Eq. (33) on the temperature change for Case 1 and $R_1 = 0.75$ is shown in Table I. In order to examine the convergence of the numerical results, the influence of the upper limit ($\equiv j_{\max}$) of series of Eq. (8) on the temperature change, displacement, stresses, electric potential and magnetic potential are shown in Table II. From the viewpoint of convergence, the numerical results in the transient state were obtained under the condition that the upper limit of series with respect to n and j are taken as $n_{\max} = 120$ and $j_{\max} = 12$.

TABLE I INFLUENCE OF THE UPPER LIMIT OF SERIES OF EQ. (33) (CASE 1, $R_1 = 0.75$)

$\tau = 0.01$, $j_{\max} = 12$	Use of Eq. (8)	Use of Eq. (33) $n_{\max} = 40$	Use of Eq. (33) $n_{\max} = 80$	Use of Eq. (33) $n_{\max} = 120$
$\bar{T}(\bar{r} = 0.7)$	2.5578E-01	2.5578E-01	2.5578E-01	2.5578E-01
$\bar{T}(\bar{r} = 0.75)$ First layer	3.1073E-01	3.1061E-01	3.1073E-01	3.1073E-01
Second layer	3.1073E-01	3.3600E-01	3.1073E-01	3.1073E-01
$\bar{T}(\bar{r} = 0.8)$ Second layer	4.0308E+00	4.5564E+00	4.0308E+00	4.0308E+00

TABLE II INFLUENCE OF THE UPPER LIMIT OF SERIES OF EQ. (8) (CASE 1, $R_1 = 0.75$)

$\tau = 0.01 \quad n_{\max} = 120$	$j_{\max} = 1$	$j_{\max} = 6$	$j_{\max} = 12$
$\bar{T}(\bar{r} = 0.7)$	2.4998E-01	2.5578E-01	2.5578E-01
$\bar{T}(\bar{r} = 0.75)$ First layer Second layer	3.0724E-01 3.0724E-01	3.1073E-01 3.1073E-01	3.1073E-01 3.1073E-01
$\bar{T}(\bar{r} = 0.8)$ Second layer Third layer	4.3183E-01 4.3183E-01	4.3080E-01 4.3080E-01	4.3080E-01 4.3080E-01
$\bar{T}(\bar{r} = 1.0)$	5.0376E-01	5.0229E-01	5.0229E-01
$\bar{u}_r(\bar{r} = 0.7)$	3.1416E-01	3.1409E-01	3.1409E-01
$\bar{u}_r(\bar{r} = 0.75)$ First layer Second layer	3.2053E-01 3.2053E-01	3.2073E-01 3.2073E-01	3.2073E-01 3.2073E-01
$\bar{u}_r(\bar{r} = 0.8)$ Second layer Third layer	3.3318E-01 3.3318E-01	3.3344E-01 3.3344E-01	3.3344E-01 3.3344E-01
$\bar{u}_r(\bar{r} = 1.0)$	4.2714E-01	4.2699E-01	4.2699E-01
$\bar{\sigma}_{rr}(\bar{r} = 0.75)$ First layer Second layer	3.8272E-03 3.8272E-03	3.2396E-03 3.2396E-03	3.2396E-03 3.2396E-03
$\bar{\sigma}_{rr}(\bar{r} = 0.8)$ Second layer Third layer	1.4562E-02 1.4562E-02	1.3906E-02 1.3906E-02	1.3906E-02 1.3906E-02
$\bar{\sigma}_{\theta\theta}(\bar{r} = 0.7)$	1.0730E-01	9.7061E-02	9.7061E-02
$\bar{\sigma}_{\theta\theta}(\bar{r} = 0.75)$ First layer Second layer	-1.7183E-02 2.5420E-01	-2.3193E-02 2.4960E-01	-2.3193E-02 2.4960E-01
$\sigma_{\theta\theta}(\bar{r} = 0.8)$ Second layer Third layer	7.9590E-02 -4.3966E-03	8.1033E-02 -2.0815E-03	8.1033E-02 -2.0815E-03
$\sigma_{\theta\theta}(\bar{r} = 1.0)$	-1.2698E-01	-1.2448E-01	-1.2448E-01
$\bar{\phi}(\bar{r} = 0.7)$	-1.2077E-03	-1.2573E-03	-1.2573E-03
$\bar{\phi}(\bar{r} = 0.75)$ First layer Second layer	1.2591E-07 1.2591E-07	1.2624E-07 1.2624E-07	1.2624E-07 1.2624E-07
$\bar{\psi}(\bar{r} = 0.7)$	-1.8855E+08	-1.8904E+08	-1.8904E+08
$\bar{\psi}(\bar{r} = 0.75)$ First layer Second layer	-1.8855E+08 -1.8855E+08	-1.8904E+08 -1.8904E+08	-1.8904E+08 -1.8904E+08

In order to confirm the results, the numerical results from this formulation are compared with those obtained using the two-layered composite hollow cylinder constructed of isotropic elastic and piezoelectric layers [26]. The variations of displacement $\bar{u}_r$, thermal stresses $\bar{\sigma}_{rr}$, $\bar{\sigma}_{\theta\theta}$ and electric potential are shown in Figs. 11(a), (b), (c) and (d), respectively. P/M/S in Fig. 11 shows the numerical results for case 1, $R_1 = 0.799$ and $R_2 = 0.8$. P/S in Fig. 11 shows the numerical results for the two-layered composite hollow cylinder constructed of isotropic elastic and piezoelectric layers which is the stacking sequence $BaTiO_3$/(mild steel) and $R_1 = 0.8$. As shown in Fig. 11, there is little difference between two analytical models.

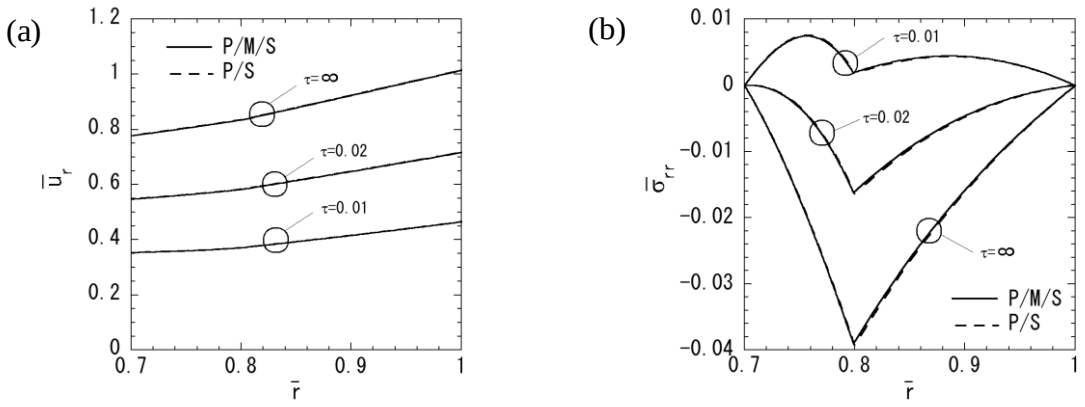

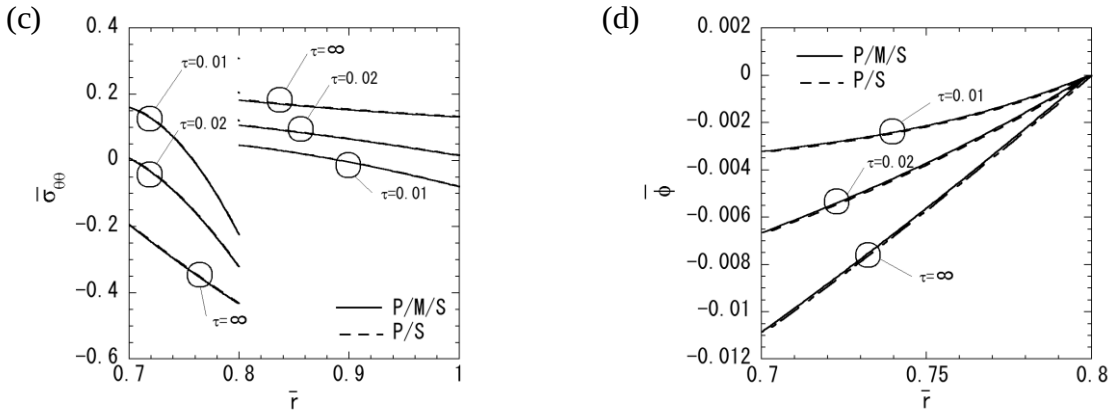

Fig. 11 Comparison between two analytical models:
(a) displacement $\bar{u}_r$, (b) normal stress $\bar{\sigma}_{rr}$, (c) normal stress $\bar{\sigma}_{\theta\theta}$ and (d) electric potential

V. CONCLUSIONS

In this study, we obtained the exact solution of the transient thermoelastic problem of a laminated hollow cylinder constructed of isotropic elastic and magneto-electro-thermoelastic materials under uniform surface heating as the plane strain state. As an illustration, we carried out numerical calculations for a three-layered hollow cylinder composed of piezoelectric and magnetostrictive materials and examined its behavior in the transient state in terms of temperature change, displacement, stress, and electric and magnetic potential distributions. Furthermore, the effects of the stacking sequence and position of the interface were investigated. Though numerical calculation was carried out for a three-layered hollow cylinder, numerical calculation for a laminated hollow cylinder constructed of isotropic elastic and magneto-electro-thermoelastic materials with an arbitrary number of layer and arbitrary stacking sequence can be carried out. The present solution can serve as a benchmark to the analysis of a laminated hollow cylinder constructed of isotropic elastic and magneto-electro-thermoelastic materials based on various numerical methods.

REFERENCES

[1] G. Harshe, J.P. Dougherty, and R.E. Newnhan, "Theoretical modeling of multilayer magnetoelectric composite," International Journal of Applied Electromagnetic in Materials, vol. 4, pp. 145-159, 1993.

[2] C.W. Nan, "Magnetoelectric effect in composites of piezoelectric and piezomagnetic phases," Physical Review B-Condensed Mater, vol. 50, pp. 6082-6088, 1994.

[3] Y. Benveniste, "Magnetoelectric effect in fibrous composites with piezoelecric and piezomagnetic Phases," Physical Review B-Condensed Mater, vol. 51, pp. 16424-16427, 1995.

[4] C.W. Nan, M.I. Bichurin, S. Dong, D. Viehland, and G. Srinivasan, "Multiferroic magnetoelectric composites: historical perspective, status, and future directions," Journal of Applied Physics, vol. 103, art. No. 031101, 2008.

[5] E. Pan, "Exact solution for simply supported and multilayered magneto-electro-elastic plates," Transaction ASME Jounal of Applied Mechanics, vol. 68, pp. 608-618, 2001.

[6] E. Pan and P.R. Heyliger, "Exact solutions for magneto-electro-elastic laminates in cylindrical bending," International Journal of Solids Structures, vol. 40, pp. 6859-6876, 2003.

[7] M.H. Babaei and Z.T. Chen, "Exact solutions for radially polarized and magnetized magnetoelectroelastic rotating cylinders," Smart Materials and Structures, vol. 17, art. No. 025035, 2008.

[8] J. Ying and H.M. Wang, "Magnetoelectroelastic fields in rotating multiferroic composite cylindrical structures," Journal of Zhejiang University Science A, vol. 10, pp. 319-326, 2009.

[9] R. Wang, Q. Han, and E. Pan, "An analytical solution for a multilayered magneto-electro-elastic circular plate under simply supported lateral boundary conditions," Smart Materials and Structures, vol. 19, art. No. 065025, 2010.

[10] H.M. Wang and H.J. Ding, "Transient responses of a magneto-electro-elastic hollow sphere for fully coupled spherically symmetric problem," European Journal of Mechanics A/Solids, vol. 25, pp. 965-980, 2006.

[11] H.M. Wang and H.J. Ding, "Radial vibration of piezoelectric/magnetostrictive composite hollow sphere," Journal of Sound and Vibration, vol. 307, pp. 330-348, 2007.

[12] R. Anandkumar, R. Annigeri, N. Ganesan, and S. Swarnamani, "Free vibration behavior of multiphase and layered magneto-electro-elastic beam," Journal of Sound and Vibration, vol. 299, pp. 44-63, 2007.

[13] D.J. Huang, H.J. Ding, and W.Q. Chen, "Static analysis of anisotropic functionally graded magneto-electro-elastic beams subjected to arbitrary loading," European Journal of Mechanics A/Solids, vol. 29, pp. 356-369, 2010.

[14] Y. Wang, R. Xu, H. Ding, and J. Chen, "Three-dimensional exact solutions for free vibrations of simply supported magnet-electro-elastic cylindrical panels," International Journal of Engineering Science, vol. 48, pp. 1778-1796, 2010.

[15] H.J. Chu, Y. Zhang, E. Pan, and Q.K. Han, "Circular surface loading on a layered multiferroic half space," Smart Materials and Structures, vol. 20, art. No. 035020, 2011.

[16] Y.T. Zhou and K.Y. Lee, "Contact proglem for magneto-electro-elastic half-plane materials indented by a moving punch, Part 1: Closed-form solutions," International Journal of Solids Structures, vol. 49, pp. 3853-3865, 2012.

[17] A. Milazzo and C. Orlando, "A beam finite element for magneto-electro-elastic multilayered composite structures," Composite Structures, vol. 94, pp. 3710-3721, 2012.

[18] C.S. Huang and C.N. Hu, "Singularity analysis for a magneto-electro-elastic body of revolution," Composite Structures, vol. 100, pp. 55-70, 2013.

[19] M. Sunar, A.Z. Al-Garni, M.H. Ali, and R. Kahraman, "Finite element modeling of thermopiezomagnetic smart structures," AIAA Journal, vol. 40, pp. 1846-1851, 2001.

[20] A. Kumaravel, N. Ganesan, and R. Sethurraman, "Steady-state analysis of a three-layered electro-magneto-elastic strip in a thermal environment," Smart Materials and Structures, vol. 16, pp. 282-295, 2007.

[21] P.F. Hou, T. Yi, and L. Wang, "2D general solution and fundamental solution for orthotropic electro-magneto-elastic materials," Journal of Thermal Stresses, vol. 31, pp. 807-822, 2008.

[22] P.F. Hou, A.Y. Leung, and H.J. Ding, "A point heat source on the surface of a semi-infinite transversely isotropic electro-magneto-thermo-elastic material," International Journal of Engineering Science, vol. 46, pp. 273-285, 2008.

[23] S.M. Xiong and G.Z. Ni, "2D green's functions for semi-infinite transversely isotropic electro-magneto-thermo-elastic composite," Journal of Magnetism Magnetic Materials, vol. 321, pp. 1867-1874, 2009.

[24] M. Rekik, S. El-Borgi, and Z. Ounaies, "The axisymmetric problem of a partially insulated mixed-mode crack embedded in a functionally graded pyro magneto-electro-elastic infinite medium subjected to thermal loading, " Journal of Thermal Stresses, vol. 35, pp. 947-975, 2012.

[25] P. Kondaiah, K. Shankar, and N. Ganesan, "Pyroelecric and pyromagnetic effects on multiphase magneto-electro-elastic cylindrical shells for axisymmetric temperature," Smart Materials and Structures, vol. 22, art. no. 025007, 2013.

[26] B.L. Wang and O.P. Niraula, "Transient thermal fracture analysis of transversely isotropic magneto-electro-elastic materials," Journal of Thermal Stresses, vol. 30, pp. 297-317, 2007.

[27] Y. Ootao and Y. Tanigawa, "Transient analysis of multilayered magneto-electro-thermoelastic strip due to nonuniform heat supply," Composite Structures, vol. 68, pp. 471-480, 2005.

[28] Y. Ootao and M. Ishihara, "Exact solution of transient thermal stress problem of a multilayered magneto-electro-thermoelasatic hollow cylinder," Journal of Solid Mechanics and Materials Engineering, vol. 5, pp. 90-103, 2011.

[29] D.A. Sarvanos and P.R. Heyliger, "Mechanics and computational models for laminated piezoelectric beams, plates, and shells," Applied Mechanics Reviews, vol. 52, pp. 305-320, 1999.

[30] T.R. Tauchert, F. Ashida, N. Noda, S. Sdali, and V. Verijenko, "Developments in thermopiezoelasticity with relevance to smart composite structures," Composite Structures, vol. 48, pp. 31-38, 2000.

[31] T.R. Tauchert and F. Ashida, "Control of transient response in intelligent piezothermoelastic structures," Journal of Thermal Stresses, vol. 26, pp. 559-582, 2003.

[32] Y. Ootao and Y. Tanigawa, "Transient piezothermoelasticity for a cylindrical composite panel composed of cross-ply and piezoelectric laminae," International Journal of Mechanical Sciences, vol. 44, pp. 1861-1877, 2002.

[33] Y. Ootao and Y. Tanigawa, "Transient piezothermoelasticity for a cylindrical composite panel composed of angle-ply and piezoelectric laminae," International Journal of Solids Structures, vol. 39, pp. 5737-5752, 2002.

[34] Y. Ootao and Y. Tanigawa, "Transient piezothermoelasticity of a two-layered composite hollow cylinder constructed of isotropic elastic and piezoelectric layers due to asymmetrical heating," Journal of Thermal Stresses, vol. 30, pp. 1003-1023, 2007.

[35] G.N. Watson, A treatise on thr theory of Bessel functions, 2nd ed., London, Cambridge University Press, pp. 40 and 63, 1980.

[36] Y. Tanigawa, T. Fukuda, Y. Ootao and S. Tanimura, "Transient thermal stress analysis of a multilayered composite laminated cylinder with a uniformly distributed heat supply and [its analytical development to nonhomogeneous materials], Transactions of the Japan Society of Mechanical Engineering, Series A, vol. 55, pp.1133-1138, 1989.

[37] Y. Ootao and Y. Tanigawa, "Control of transient thermoelastic displacement of a two-layered composite plate constructed of isotropic elastic and piezoelectric layers due to nonuniform heating," Archive of Applied Mechanics, vol. 71, pp. 207-220, 2001.